Homo- and Heteroannularly Bridged Ferrocenyl Diphosphines in Asymmetric Hydrogenations

Thomas Sturm and Walter Weissensteiner*,†

Institut für Organische Chemie, Universität Wien, Währinger Strasse 38, A-1090 Wien, Austria

Felix Spindler*

Solvias AG, Catalysis Research, P. O. Box, CH-4002 Basel, Switzerland

Kurt Mereiter

Institute of Mineralogy, Crystallography and Structural Chemistry, Vienna University of Technology, Getreidemarkt 9, A-1060 Vienna, Austria

Ana M. López-Agenjo, Blanca R. Manzano, and Félix A. Jalón*

Facultad de Químicas, Universidad de Castilla-La Mancha, Avenida Camilo J. Cela 10, E-13071 Ciudad Real, Spain

Received August 14, 2001

Four new enantiopure homo- and heteroannularly bridged ferrocenyl diphosphine ligands have been synthesized, characterized, and tested in enantioselective hydrogenations of olefins [methyl-(*Z*)-(α)-(acetamido)cinnamate, (*Z*)-(α)-methylcinnamic acid and dimethyl itaconate], ketones (ethyl pyruvate, methyl phenylglyoxylate, and ketopantolactone), and the imine 2-ethyl-*N*-(2-methoxy-1-methylethylidene)-6-methylbenzeneamine (MEAI). Generally, the homoannularly bridged ligand (S_c,R_p)-[η^5-cyclopentadienyl][η^5-4-dicyclohexylphosphino-3-diphenylphosphino-4,5,6,7-tetrahydro-1*H*-indenyl]iron(II) performed best, giving up to 90.6% ee in the rhodium-catalyzed hydrogenation of dimethyl itaconate and 73% ee in the iridium-catalyzed hydrogenation of MEAI. The molecular structures of all new ligands in the solid state have been determined by X-ray diffraction. A structural comparison of the four new diphosphines with Josiphos-type ligands revealed that the stiffness of the ligand backbone strongly influences the enantioselectivity observed.

Introduction

Chiral ferrocenyldiphosphines constitute a class of ligands that give outstanding performance in asymmetric catalysts,[1] and among these systems, Josiphos[2] and Xyliphos[3] are the most prominent examples (Chart 1). Generally, the success of this class of compounds has been attributed to the fact that fine-tuning of the ligands to different metals and substrates is easily achieved by functional group variation, a synthetic process essentially limited only by the availability of appropriate phosphines.[2]

Among the small number of Josiphos-type ligands[4] that are used industrially [i.e., Xyliphos, Josiphos (**I**), and PPF-tBu_2], Josiphos was found to be particularly interesting since—like BINAP—it has been successfully employed not only for different substrates but also for a wide range of asymmetric reactions including hydrogenations,[2,3a,5] hydroborations,[2a] allylic alkylations,[2,6] polymerizations,[7] and others.[3b,4e,8] For ligands with such

† E-mail: Walter.Weissensteiner@univie.ac.at.

(1) *Ferrocenes, Homogeneous Catalysis, Organic Synthesis, Material Science*; Togni, A., Hayashi, T., Eds.; VCH: Weinheim, 1995. *Catalytic Asymmetric Synthesis*, Ojima, I., Ed.; Wiley-VCH: New York, 2000.

(2) Togni, A.; Breutel, C.; Schnyder, A.; Spindler, F.; Landert, H.; Tijani, A. *J. Am. Chem. Soc.* **1994**, *116*, 4062. (b) Togni, A.; Spindler, F.; Zanetti, N.; Tijani, A. (Ciba-Geigy A.-G., Switz.) Eur. Pat. Appl. EP 564406 A1 19931006, 1993.

(3) Spindler, F.; Pugin, B.; Jalett, H.-P.; Buser, H.-P.; Pittelkow, U.; Blaser, H.-U. *Chem. Ind.* (Dekker) **1996**, *68* (Catalysis of Organic Reactions), 153. (b) Dorta, R.; Egli, P.; Zuercher, F.; Togni, A. *J. Am. Chem. Soc.* **1997**, *119*, 10857. (c) Spindler, F.; Pugin, B.; Buser, H.; Jalett, H.-P.; Pittelkow, U.; Blaser, H.-U. *Pestic. Sci.* **1998**, *54*, 302. (d) Dorta, R.; Togni, A. *Organometallics* **1998**, *17*, 3423. (e) Blaser, H.-U.; Buser, H.-P.; Jalett, H.-P.; Pugin, B.; Spindler, F. *Synlett* **1999**, 867; Rampf, F. A.; Herrmann, W. A. *J. Organomet. Chem.* **2000**, *601*, 138.

(4) Jalett, H.-P.; Spindler, F.; Blaser, H.-U.; Hanreich, R. G. (Ciba-Geigy A.-G., Switz.) PCT Int. Appl. WO 9521151 A1 19950810, 1995. (b) Jalett, H.-P.; Spindler, F.; Hanreich, R. G. (Ciba-Geigy A.-G., Switz.) PCT Int. Appl. WO 9641793 A1 19961227, 1996. (c) Jalett, H.-P.; Siebenhaar, B. (Ciba-Geigy A.-G., Switz.) PCT Int. Appl. WO 9705095 A1 19970213, 1996. (d) Sablong, R.; Osborn, J. A.; Spindler, F. (Ciba-Geigy A.-G., Switz.) PCT Int. Appl. WO 9705094 A1 19970213, 1996. (e) Bieler, N.; Egli, P.; Dorta, R.; Togni, A.; Eyer, M. (Lonza A.-G., Switz.) Eur. Pat. Appl. EP 909762 A2 19990421, 1998.

(5) Zanetti, N. C.; Spindler, F.; Spencer, J.; Togni, A.; Rihs, G. *Organometallics* **1996**, *15*, 860. (b) Werbitzky, O. (Lonza A.-G., Switz.) PCT Int. Appl. WO 9703052 A1 19970130, 1996. (c) Fuchs, R. (Lonza A.-G., Switz.) Eur. Pat. Appl. EP 803502 A2 19971029, 1997. (d) Akotsi, O. M.; Metera, K.; Reid, R. D.; Mcdonald, R.; Bergens, S. H. *Chirality* **2000**, *12*, 514.

10.1021/om0107439 CCC: $22.00
Publication on Web 04/04/2002

Chart 1

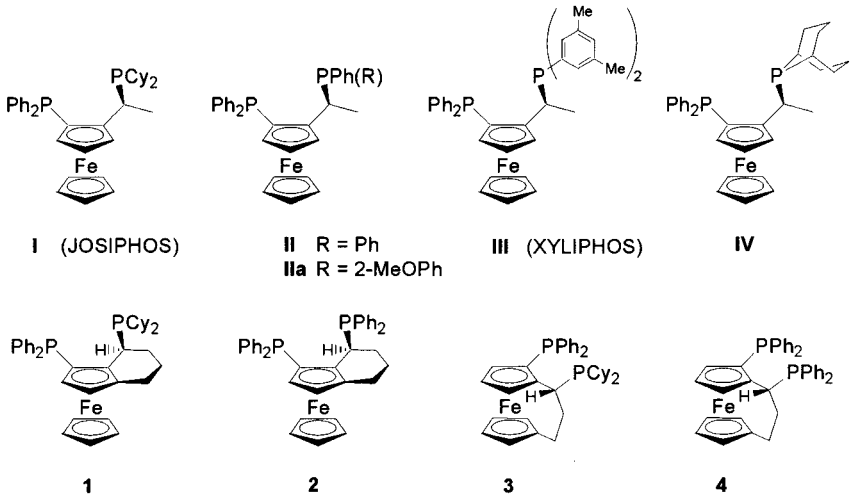

a broad applicability it is certain that a number of steric and electronic properties must combine extremely well in order to give both high yields and high (enantio)-selectivities. Recently, we questioned whether conformational flexibility could be one such parameter.[9] One might imagine that in the formation of transition metal complexes with Josiphos-type diphosphines the flexibility of the ethyl side chain—in particular the fact that the whole unit can rotate freely about the C(Fc)—C(P) single bond—contributes significantly to the necessary ligand adjustment. Therefore, in addition to an investigation into new types of diphosphine ligands, it seemed to be of interest to study the influence of a reduced conformational flexibility on enantioselectivity (stiff versus flexible ligand backbones) by changing the mobile side chain of Josiphos-type ligands to a much less flexible homo- or heteroannular bridge.

We report here the synthesis of four homo- and heteroannularly bridged ferrocenyl diphosphines, **1**−**4**, all of which are related to either Josiphos, **I**, or its bis-diphenylphosphino analogue **II** (Chart 1). In addition, structural features of these new ligands are described, along with a number of catalysis results obtained in different asymmetric hydrogenation reactions, and the data obtained compared to those of Josiphos and related ligands.

Scheme 1

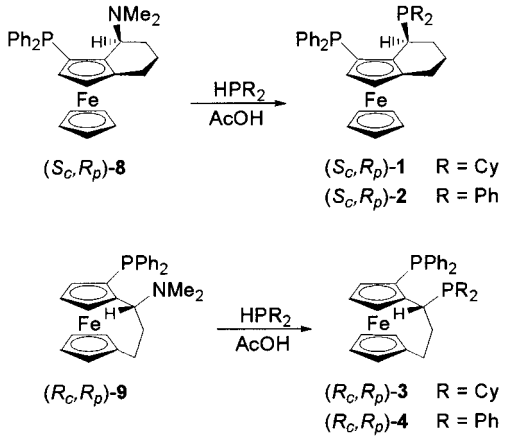

Results and Discussion

Synthesis of Diphosphines 1−4. Both enantiomers of the homo- and heteroannularly bridged ligands **1**−**4** were easily accessible from the appropriate aminophosphine **8** or **9**. The route is shown in Scheme 1 for one enantiomer only.

Reaction of enantiopure aminophosphines (S_c,R_p)-**8** or (R_c,R_p)-**9** with either diphenyl- or dicyclohexylphosphine in acetic acid gave diphosphines (S_c,R_p)-**1** (68%) and (S_c,R_p)-**2** (68%) or (R_c,R_p)-**3** (78%) and (R_c,R_p)-**4** (86%), respectively. In each case the reaction proceeded with retention of configuration. The synthesis of aminophosphine (R_c,R_p)-**9**[10] and the homoannularly bridged enantiopure (R_p)-**5**,[11] the precursor of aminophosphine (S_c,R_p)-**8** (Scheme 2), has previously been described by our group. Reduction of (R_p)-**5** with $LiAlH_4$ gave alcohol (S_c,R_p)-**6** (98%), which was subsequently transformed with $HNMe_2/AlCl_3$ into amine (S_c,R_p)-**7** in 74% yield. Finally, treatment of this compound with *n*-BuLi and quenching with chlorodiphenylphosphine led to the desired aminophosphine (S_c,R_p)-**8** (71%). It should be mentioned that diphosphines **1** and **2** are accessible not

(6) Breutel, C.; Pregosin, P. S.; Salzmann, R.; Togni, A. *J. Am. Chem. Soc.* **1994**, *116*, 4067. (b) Pregosin, P. S.; Salzmann, R.; Togni, A. *Organometallics* **1995**, *14*, 842. (c) Barbaro, P.; Pregosin, P. S.; Salzmann, R.; Albinati, A.; Kunz, R. *Organometallics* **1995**, *14*, 5160.

(7) Bronco, S.; Consiglio, G.; Di Benedetto, S.; Fehr, M.; Spindler, F.; Togni, A. *Helv. Chim. Acta* **1995**, *78*, 883. (b) Bronco, S.; Consiglio, G.; Di Benedetto, S.; Drent, E. (Shell Internationale Research Maatschappij B.V., Neth.) Brit. UK Pat. Appl. GB 2289855 A1 19951206, 1994. (c) Broekhoven, J. A. M.; Drent, E.; Reynhout, M. J. (Shell Internationale Research Matschappij B.V., Neth.) Brit. UK Pat. Appl. GB 2289895 A1 19951206, 1994. (d) Gambs, C.; Chaloupka, S.; Consiglio, G.; Togni, A. *Angew. Chem., Int. Ed.* **2000**, *39*, 2486.

(8) Shaughnessy, K. H.; Kim, P.; Hartwig, J. F. *J. Am. Chem. Soc.* **1999**, *121*, 2123. (b) Botteghi, C.; Delogu, G.; Marchetti, M.; Paganelli, S.; Sechi, B. *J. Mol. Catal. A: Chem.* **1999**, *143*, 311. (c) Sperrle, M.; Consiglio, G. *J. Mol. Catal. A: Chem.* **1999**, *143*, 263. (d) Chapuis, C.; Barthe, M (Firmenich S. A., Switz.) Eur. Pat. Appl. EP 949241 A2 19991013 EP, 1999. (e) Buchwald, S.; Old, D. W.; Wolfe, J. P.; Palucki, M.; Kamikawa, K.; Chieffi, A.; Sadighi, J. P.; Singer, R. A.; Ahman, J. PCT Int. Appl. WO 2000002887 A2 20000120, 1999. (f) Rampf, F. A.; Herrmann, W. A. *J. Organomet. Chem.* **2000**, *601*, 138.

(9) Jedlicka, B.; Kratky, C.; Weissensteiner, W.; Widhalm, M. *J. Chem. Soc., Chem. Commun.* **1993**, *17*, 1329. (b) Wally, H.; Widhalm, M.; Weissensteiner, W.; Schlögl, K. *Tetrahedron: Asymmetry* **1993**, *4*, 285. (c) Wally, H.; Kratky, C.; Weissensteiner, W.; Widhalm, M.; Schlögl, K. *J. Organomet. Chem.* **1993**, *450*, 185.

(10) Mernyi, A.; Kratky, C.; Weissensteiner, W.; Widhalm, M. *J. Organomet. Chem.* **1996**, *508*, 209. (b) Cayuela, E. M.; Xiao, L.; Sturm, T.; Manzano, B. R.; Jalon, F. A.; Weissensteiner, W. *Tetrahedron: Asymmetry* **2000**, *11*, 861.

(11) Wally, H.; Nettekoven, U.; Weissensteiner, W.; Werner, A.; Widhalm, M. *Enantiomer* **1997**, *2*, 441.

Scheme 2

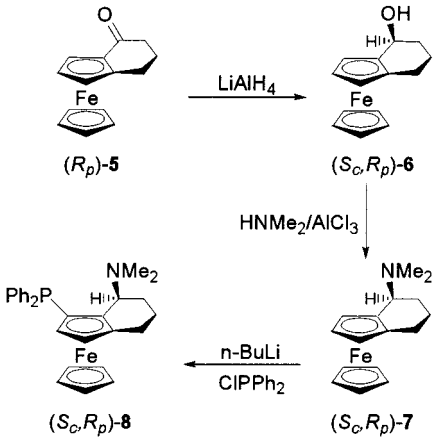

only from (S_c,R_p)-**8** (Scheme 1) but also from its diastereomer (R_c,R_p)-**8**[12a] (PTFA), although this alternative route leads to significantly lower yields.

Solid-State Structures of Ligands 1−4. The molecular structures of all four ligands were determined by X-ray diffraction. Details of the X-ray crystallography techniques are given in the Experimental Section. The following enantiomers were used and are depicted in Figure 1: (R_c,S_p)-**1**, (R_c,S_p)-**2**, (S_c,S_p)-**3**, and (R_c,R_p)-**4**. The absolute structure of each compound was determined from the X-ray anomalous dispersion effects and was consistent with the chemical evidence.

Compounds **2**−**4** crystallized with one molecule per asymmetric unit, whereas **1** crystallized with two independent molecules per asymmetric unit. The overall structural features of **1**−**4** are similar to those of other related homo- and heteroannularly bridged derivatives such as (R_c,R_p)-**8**[12a] or (S_c,S_p)-**9**.[10] The heteroannular bridge in **3** and **4** imposes considerable strain on the ferrocene unit, which leads to a significant tilt of the cyclopentadienyl groups with tilt angles of 8.4° (**3**) and 8.8° (**4**). The strain also leads to out-of-plane deformations of the bridge carbons C(1) and C(3) toward the iron-coordinated Cp-sides [**3**: C(1) 0.13 Å, C(3) 0.17 Å; **4**: C(1) 0.11 Å, C(3) 0.18 Å]. Such deformations are much less pronounced in derivatives **1** and **2**. The bond lengths and bond angles of all ferrocene units are within the expected range. In analogy to the structure of **9**,[10] the bridge carbon C(2) in ligands **3** and **4** is located in close proximity to the diphenylphosphino group attached to the Cp ring. This situation forces the C(1)−P(2) bond to point in a direction perpendicular to the plane of the Cp^1 ring [Cp^1: C(21)−C(25); torsion angles P(2)−C(1)−C(21)−C(25): 121.1° (**3**), 128.4° (**4**)]. As one might expect, the phosphino groups attached to the homoannular bridge in ligands **1** and **2** adopt a pseudoequatorial position. As mentioned above, two molecules (**1A** and **1B**) per asymmetric unit were found for compound **1**. A comparison of these independent structures shows a similar overall conformation but very significant differences concerning the dicyclohexylphosphino unit (for a superposition of both molecules see Figure 2).

As compared to **1A** the whole dicyclohexylphosphino unit of **1B** is positioned higher above Cp^1, resulting in a decrease of the torsion angle P(2)−C(1)−C(21)−C(25) (**1A**: 147.3°, **1B**: 129.1°) and in an increased normal distance of P(2) from Cp^1 (**1A**: 0.92 Å, **1B**: 1.49 Å above Cp^1). It is interesting to note that in all ligands the phosphino groups are already well preorganized for complexation to a transition metal, with both phosphino lone pairs already pointing toward each other.

Conformational Variability. The following discussion addresses the differences in the backbone flexibility of Josiphos-type ligands as compared to diphosphines **1**−**4** (Chart 1). Josiphos-type diphosphines are expected to be rather flexible, particularly with respect to a rotation of the phosphinoethyl unit about the CH(P)−C(Fc) single bond [corresponding to bond C(1)−C(21) of ligands **1**−**4**]. On forming transition metal complexes, this feature, regardless of other factors, should allow the ligands to adjust easily not only to different metals but also to changing oxidation states, geometries, and substitution patterns—changes that typically occur during the course of a catalytic cycle. Experimental evidence to support this view comes from a number of X-ray structures, most of which involve ligands **I**−**IV** (Chart 1). A closer look at the molecular structures of diphosphines **I**,[13] **IIa**,[13] and **IV**[14] shows that their side chain orientation strongly depends on the phosphorus substituents, with torsion angles P−CH(P)−C(Fc)−CH(Fc) [corresponding to torsion angles P(2)−C(1)−C(21)−C(25) in **1**−**4**] ranging from 50.4° to 107.8° (**I**: 107.8°, **IIa**: 103.9°, **IV**: 50.4°). More important, however, is the question of how these ligands react upon complexation to transition metals. In general, a number of conformational changes are involved: (i) rotation of both phosphino groups about the P−C(Fc) and P−CH(Fc) bonds [P(1)−C(22) and P(2)−C(1) in **1**−**4**], respectively, (ii) rotation of the side chain about CH(P)−C(Fc) [C(1)−C(21) in **1**−**4**], (iii) rotation of all phosphorus substituents, and (iv) out-of-plane deformations. Complexation of Josiphos-type ligands leads to a situation where adjustment of the ethyl side chain and of the attached phosphino unit play a predominant role. For example, in Rh,[13] Ru,[15] Pd,[13] and Pt[13] complexes of Josiphos the side chain torsion angle covers a range from 111.1° to 130.2°. For the Ir complexes of Xyliphos,[16] angles in the range 133.5−137.5° were found. The most spectacular changes, however, involve ligands **II** and **IV**. The reported Ir complexes of **II**[17] have angles in the range 133.5−142.4° but also from −151.1° to −156.5°, meaning that in the latter case the phosphorus attached to the side chain is actually located below Cp^1, an arrangement also found for both Pd-allyl complexes of **IV**.[15] On the basis of the X-ray data, the phosphinoethyl unit of all the Josiphos-type ligands under discussion has a large amount of space available upon rotation of the C(P)−C(Fc) single bond.

Very little information is available about the conformational properties of ligands **1**−**4**, and we therefore

(12) Jedlicka, B. Doctoral Thesis, University of Vienna, Austria, 1995. (b) Sturm, T.; Doctoral Thesis, University of Vienna, Austria, 2000.

(13) Togni, A.; Breutel, C.; Soares, M. C.; Zanetti, N.; Gerfin, T.; Gramlich, V.; Spindler, F.; Rihs, G. *Inorg. Chim. Acta* **1994**, *222*, 213.

(14) Abbenhuis, H. C. L.; Burckhardt, U.; Gramlich, V.; Kollner, C.; Pregosin, P. S.; Salzmann, R.; Togni, A. *Organometallics* **1995**, *14*, 759.

(15) Zanetti, N. C.; Spindler, F.; Spencer, J.; Togni, A.; Rihs, G. *Organometallics* **1996**, *15*, 860.

(16) Dorta, R.; Togni, A. *Organometallics* **1998**, *17*, 5441.

(17) Dorta, R.; Togni, A. *Organometallics* **1998**, *17*, 3423.

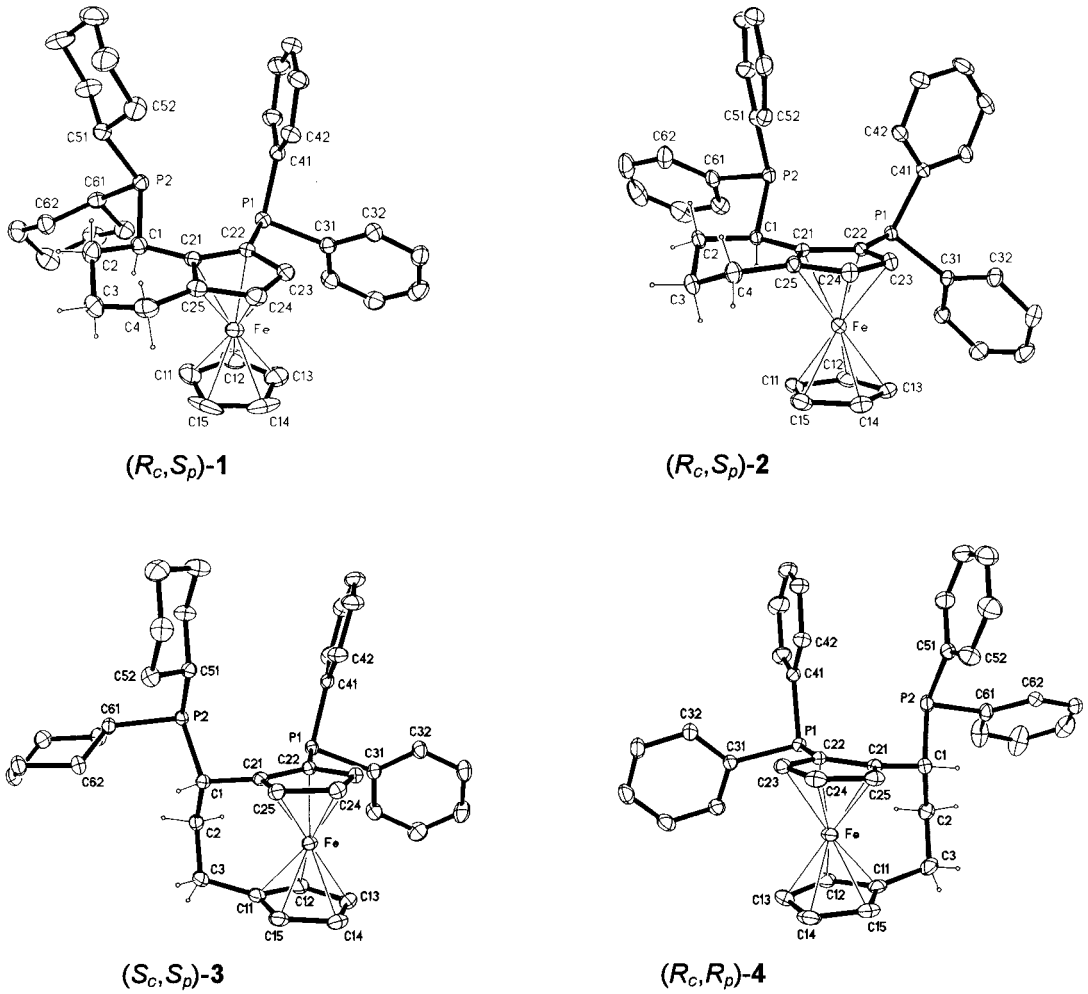

Figure 1. Molecular structures of (R_c,S_p)-**1** (molecule **1A**), (R_c,S_p)-**2**, (S_c,S_p)-**3**, and (R_c,R_p)-**4** in the solid state. Aromatic and cyclohexyl hydrogens omitted for clarity.

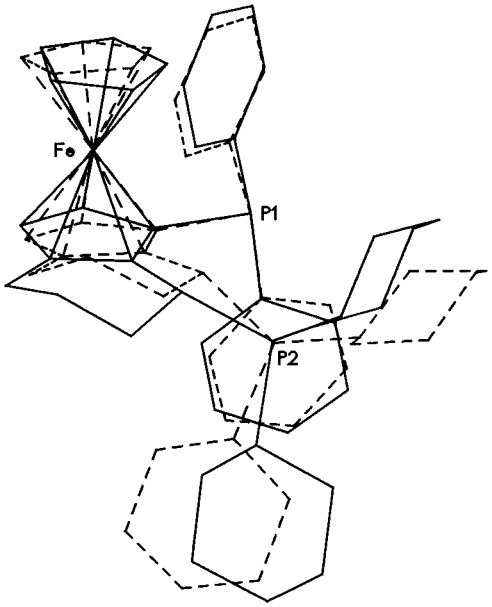

Figure 2. Superposition plot of the two independent molecules **1A** (full lines) and **1B** (broken lines) in crystalline (R_c,S_p)-**1**. Fe and P atoms were used to fit the two molecules.

decided to carry out force field calculations.[18] Within the known limits,[10] the solid-state structures of **1**−**4** were reproduced reasonably well and, with the exception of **4**, were found to represent the conformers of lowest energy (in the case of **1**, where two different molecules are present in the crystal lattice, the calculated structure fits molecule **1A** significantly better than **1B**, see Figure 1). In the case of **4**, a slightly more stable conformer (by 0.4 kcal/mol) was located, and this has a different arrangement of the phenyl rings of the phosphino unit attached to the heteroannular bridge. In principle, depending on the conformation of the homo- or heteroannular bridge, two conformers should be accessible for each ligand (Scheme 3).

For the two homoannular ligands (**1** and **2**) the pseudo-equatorial conformer (a) was calculated to be of lowest energy while the pseudo-axial arrangement (b) is slightly less stable [**1**: 1.2 kcal/mol; **2**: 1.6 kcal/mol; torsion angles P(2)−C(1)−C(21)−C(25) of 126.3° (*ax*-**1**) and 122.6° (*ax*-**2**)]. These energy differences are much more pronounced for the heteroannular ligands **3** and **4**. According to the calculations, conformers (b) (Scheme 3, bottom) are higher in energy by 7.8 kcal/mol (**3**) and 4.6 kcal/mol (**4**). On the basis of these calculated energy differences, we expect ligands **1** and **2** to be present in solution as a mixture of conformers (a) and (b), while for ligands **3** and **4** conformer (b) can be excluded. This

(18) PCMODEL V 7.0; Serena Software, Box 3076, Bloomington, IN 47402−3076.

Scheme 3. Ground State (a) and Higher Energy (b) Conformers of Ligands 1, 2 (top) and 3, 4 (bottom)

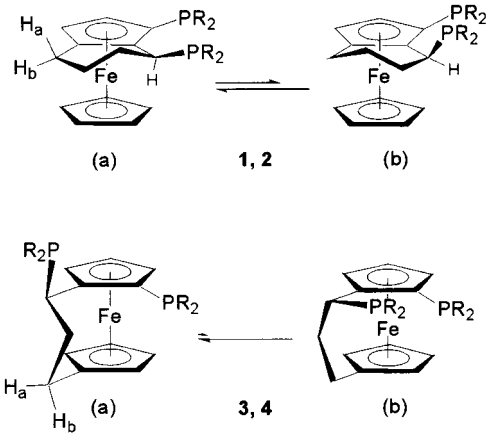

view is also supported by the results of an analysis of the vicinal coupling constants of bridge protons H_a and H_b of ligands **1**, **2**, and **4** (in the case of **3** these resonances are obscured by cyclohexyl protons; for H_a and H_b see Scheme 3). Ligand **4** shows coupling constants of 14.0 Hz and <1 Hz (H_a, 1.6 ppm, see Experimental Section) as well as 4.0 and 2.5 Hz (H_b, 2.46 ppm), and these values are in the expected range for one predominant conformer [(a), Scheme 3]. The coupling constants measured for the homo-annularly bridged diphosphines **1** and **2** [i.e., 10.0, 5.5 Hz (H_a, 2.27 ppm) and 5.0, 5.0 Hz (H_b, 2.59 ppm) for **1**, and 8.9, 5.9 Hz (H_a, 2.16 ppm) and 4.5, 4.5 Hz (H_b, 2.55 ppm) for **2**] are intermediate with respect to those calculated for conformers (a) and (b).[18] These values indicate a mixture of conformers in which one predominates. On the basis of both the calculated energy differences and the NMR data, it is reasonable to assume that in transition metal complexes ligands **1** and **2** can adopt both pseudo-equatorial and pseudo-axial conformations, while for complexes of **3** and **4** a ligand conformation such as (b) (Scheme 3) can be excluded. Experimental data are only available for the $PtCl_2$ complexes of **3** and **4**[19] and a Pd-(1,3-diphenylallyl) complex of **1**.[12b] In the $PtCl_2$ complexes, the ligand backbones are essentially unchanged in comparison to the solid-state structures of **3** and **4** [torsion angles P(2)−C(1)−C(21)−C(25) for **3**·$PtCl_2$: 123.6°; **3**: 121.1°; **4**·$PtCl_2$: 127.2°; **4**: 128.4°], while in the complex [**1**·Pd(1,3-diphenylallyl)]CF_3SO_3 ligand **1** adopts a pseudo-equatorial conformation similar to that of **1B** [torsion angle P(2)−C(1)−C(21)−C(25): 125.2°; **1A**: 147.3°; **1B**: 129.1°]. From both the experimental data and calculations it is clear that the accessible space for the side chain phosphino units in Josiphos-type ligands is much larger than that in ligands **1**−**4**, with ligands **3** and **4** being much more rigid than **1** and **2**.

Hydrogenations. In performing the hydrogenation reactions[20] we primarily focused on two aspects: (i) the scope and overall performance of complexes of ligands **1**−**4** and (ii) their (enantio)selectivity as compared to the structurally closely related Josiphos (**I**) and, in a few cases, its bis(diphenylphosphino) analogue **II**. Different types of substrates—olefins, ketones and one imine—were selected to cover a wide range of structural motives (Chart 2). All reactions were carried out with rhodium or iridium catalysts prepared in situ.

Hydrogenation of Olefins. The hydrogenations of methyl (*Z*)-(α)-(acetamido)cinnamate (MAC), (*Z*)-(α)-methylcinnamic acid (MCA), and dimethyl itaconate (DMI) (see Chart 2) were all performed in MeOH at low hydrogen pressure and at low to moderate temperature (up to 40 °C). In all cases the catalyst was prepared in situ by reacting $[Rh(COD)_2]BF_4$ with the appropriate ligand. With a few exceptions, a substrate-to-catalyst ratio of 200 was chosen. The results are summarized in Table 1. The conversion was always close to 100%, except in the case where MCA was used as the substrate, although enantioselectivities varied markedly. Ligand **1** gave the best results with all three substrates. An increase in the ee was observed upon lowering the reaction temperature. For example, with DMI and ligand **1** the ee increased from 86% at 18 °C to 90.6% at −10 °C (entries 15−17) and with **3** from 60.1% to 66.7% (35 °C to 15 °C, entries 19−21). The best result in terms of ee was obtained in the hydrogenation of DMI at −10 °C using ligand **1** (entry 17).

Hydrogenation of Ketones. Rhodium-catalyzed hydrogenations of the ketones ethyl pyruvate (ETPY), methyl phenylglyoxylate (MPG), and ketopantolactone (KPL) (Chart 2) usually require higher pressure and were carried out in toluene with a hydrogen pressure of 40(50) or 80 bar, again with Rh catalysts prepared in situ. Depending on the substrate, precursors $[(NBD)RhCl]_2$ (ETPY and MPG) and $[(NBD)Rh(OAc)]_2$ (KPL) were used. A summary of all results is listed in Table 2. Generally, ligands **1**−**4** gave only moderate results with a maximum ee of 57% for ligand **3** with KPL as the substrate (entry 42). Both conversion and enantioselectivity are strongly dependent on pressure. For example, in the hydrogenation of KPL with ligand **1** (entries 38 and 39), lowering the hydrogen pressure from 80 to 50 bar changed the enantioselectivity from 54.9% to <5% ee. A comparable change is also observed with ligand **3** and KPL (entries 41 and 42). With all substrates the conversion is significantly higher with the dicyclohexylphosphino ligands **1** and **3** as compared to the bis(diphenylphosphino) ligands **2** and **4** (see Table 2: entries 28 and 30, 32 and 34, 38 and 40 as well 41 and 43). In addition, a very pronounced solvent dependence was observed (entries 32 and 33).

Hydrogenation of Imine MEAI. As a test substrate for an iridium-catalyzed imine reduction the commercially important 2-ethyl-*N*-(2-methoxy-1-methylethylidene)-6-methylbenzeneamine (MEAI) was chosen. In this case, $[(COD)IrCl]_2$ was used as the catalyst precursor. All reactions were carried out in toluene at a hydrogen pressure of 80 bar. Total conversion was reached within 18 h except in the case of ligand **3**.

(19) Sturm, T.; Weissensteiner, W.; Mereiter, K.; Kegl, T.; Jeges, G.; Petolz, G.; Kollar, L. *J. Organomet. Chem*. **2000**, *595*, 93.

(20) For recent overviews on asymmetric hydrogenations see: (a) Ohkuma, T.; Kitamura, M.; Noyori, R. Asymmetric Hydrogenation. In *Catalytic Asymmetric Synthesis*; Ojima, I., Ed.; Wiley-VCH: New York, 2000; p 1. (b) Brown, J. M. Hydrogenation of Functionalized Carbon−Carbon Double Bonds. In *Comprehensive Asymmetric Catalysis Vol. I−III*; Jacobsen, E. N., Pfaltz, A., Yamamoto, H., Eds.; Springer: Berlin, 1999; p 121. (c) Ohkuma, T.; Noyori, R. Hydrogenation of Carbonyl Groups. In *Comprehensive Asymmetric Catalysis Vol. I−III*; Jacobsen, E. N., Pfaltz, A., Yamamoto, H., Eds.; Springer: Berlin, 1999; p 199. (d) Blaser, H.-U.; Spindler, F. Hydrogenation of Imino Groups. In *Comprehensive Asymmetric Catalysis Vol. I−III*; Jacobsen, E. N., Pfaltz, A., Yamamoto, H., Eds.; Springer: Berlin, 1999; p 247.

Chart 2

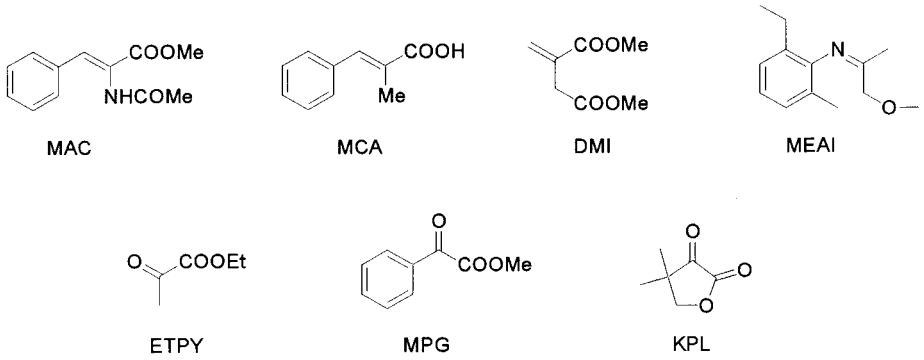

Table 1. Rhodium-Catalyzed Hydrogenation of Olefins MAC, MCA, and DMI

entry	substrate	ligand	$p(H_2)$ [bar]	T [°C]	time [h]	conv [%]	ee [%]	config
1	MAC[a,b]	(R_c,S_p)-**I**	1	18	66	100	84.4	(*S*)
2		(R_c,S_p)-**1**	1	18	20	98.7	71.1	(*S*)
3		(R_c,S_p)-**2**	5	40	64	99.5	61	(*S*)
4		(R_c,S_p)-**2**	1	18	20	100	21.6	(*S*)
5		(R_c,R_p)-**3**	1	25	64	95	35	(*S*)
6		(R_c,R_p)-**4**	5	35	18	100	7	(*S*)
7		(R_c,R_p)-**4**	1	18	19	100	11.8	(*S*)
8	MCA[a,c]	(R_c,S_p)-**I**	6	25	16.5	100	25.1	(*S*)
9[d]		(R_c,S_p)-**1**	6	25	16	20	55	(*S*)
10		(R_c,S_p)-**2**	6	25	18	84	2.3	(*S*)
11		(R_c,R_p)-**3**	6	25	18	100	32.3	(*S*)
12		(R_c,R_p)-**4**	6	25	66	42	26.1	(*S*)
13	DMI[a,e]	(R_c,S_p)-**I**	1	18	22	100	98.5	(*S*)
14		(R_c,S_p)-**II**	1	18	19	100	96.7	(*S*)
15		(R_c,S_p)-**1**	1	18	18	100	86	(*S*)
16		(R_c,S_p)-**1**	1	3	19	100	89.4	(*S*)
17		(R_c,S_p)-**1**	1	−10	18	100	90.6	(*S*)
18		(R_c,S_p)-**2**	1	18	66	100	83.2	(*S*)
19		(R_c,R_p)-**3**	1	35	20	100	60.1	(*S*)
20		(R_c,R_p)-**3**	1	18	63	100	63.3	(*S*)
21[f]		(R_c,R_p)-**3**	1	15	21	100	66.7	(*S*)
22		(R_c,R_p)-**4**	1	18	18	100	42.8	(*S*)

[a] MAC, MCA, DMI catalyst precursor: $[(NBD)_2Rh]BF_4$; S/C = 200; solvent: methanol. [b] ee determination by GC on Lipodex-E (He carrier, 95 °C, isothermic). [c] ee determination by HPLC on Chiralcel OB (Daicel; eluent: hexane/2-propanol = 97/3, flow: 0.1 mL/min). [d] S/C = 100. [e] ee determination by GC on Lipodex-E (He carrier, 100 °C, isothermic). [f] S/C = 155.

Table 2. Rhodium-Catalyzed Hydrogenation of Ketones ETPY, MPG, and KPL

entry	substrate	ligand	$p(H_2)$ [bar]	T [°C]	time [h]	conv [%]	ee [%]	config
23	ETPY[a]	(R_c,S_p)-**I**	80	0	16	77	49.5	(*R*)
24		(R_c,S_p)-**II**	80	0	67	14	9.1	(*R*)
25[b]		(R_c,S_p)-**1**	80	10	19	32	15.7	(*R*)
26		(R_c,S_p)-**1**	80	0−5	18	72	41.7	(*R*)
27		(R_c,S_p)-**1**	80	0	16	38	40.6	(*R*)
28		(R_c,S_p)-**1**	40	25	19	93	44	(*R*)
29		(R_c,S_p)-**2**	80	0	67	18	6.2	(*R*)
30		(R_c,S_p)-**2**	40	25	19	32	50	(*R*)
31[c]		(R_c,R_p)-**3**	40	25	18	50	50	(*R*)
32	MPG[e]	(R_c,S_p)-**1**	40	25	16	78	13	(*R*)
33[b]		(R_c,S_p)-**1**	40	25	18	<5	n.d.[g]	
34		(R_c,S_p)-**2**	40	25	16	<5	n.d.[g]	
35[c,d]		(R_c,R_p)-**3**	40	25	18	8	34	(*R*)
36	KPL[f]	(R_c,S_p)-**I**	80	20	16	50	32.6	(*R*)
37		(R_c,S_p)-**II**	80	20	16.5	17	6.3	(*R*)
38		(R_c,S_p)-**1**	80	20	18	96	54.9	(*R*)
39[d]		(R_c,S_p)-**1**	50	25	18	100	<5	
40		(R_c,S_p)-**2**	80	20	18	31	44.7	(*R*)
41		(R_c,R_p)-**3**	80	20	16.5	56	16.5	(*R*)
42[d]		(R_c,R_p)-**3**	50	25	16	70	57	(*R*)
43		(R_c,R_p)-**4**	80	20	16.5	<5	n.d.[g]	

[a] ETPY; catalyst precursor (except entry 31): $[(NBD)RhCl]_2$; S/C = 200; solvent: toluene; ee determination on Lipodex-E (He carrier, 95 °C, isothermic). [b] Solvent: toluene/MeOH, 1/1. [c] Catalyst precursor: [(NBD)Rh(OTFA)]. [d] S/C = 100. [e] MPG: catalyst precursor (except entry 35): $[NBD)RhCl]_2$; S/C = 200; solvent: toluene; ee determination on Lipodex-A (H_2 carrier, 120 °C, isothermic). [f] KPL: catalyst precursor: [(NBD)Rh(OAc)]; S/C = 200; solvent: toluene; ee determination on Lipodex-E (He carrier, 160 °C, isothermic). [g] Not determined because of low conversion.

Table 3. Iridium-Catalyzed Hydrogenation of Imine MEAI[a]

entry	ligand	$p(H_2)$ [bar]	T [°C]	time [h]	conv [%]	ee [%]	config
45	(R_c,S_p)-**I**	80	25	19	80	73	(*R*)
46	(R_c,S_p)-**1**	80	25	18	100	73	(*R*)
47	(R_c,S_p)-**2**	80	25	18	100	73	(*R*)
48	(R_c,R_p)-**3**	80	25	18	53	32	(*R*)
49	(R_c,R_p)-**4**	80	25	18	100	0	

[a] Catalyst precursor: $[(COD)IrCl]_2$; S/C: 1000; solvent: toluene; ee determined by HPLC on Chiralcel OD (Daicel; eluent: hexane/2-propanol = 99.6/0.4, flow: 1.0 mL/min).

Again, the homoannularly bridged ligands **1** and **2** performed better than **3** and **4**, reaching a respectable enantioselectivity of 73% (Table 3), which is almost equal to the value obtained with the commercially used Xyliphos (79%).

Comparison of Ligands 1−4 with Josiphos. To make a more direct comparison, the enantioselectivities obtained with ligands **I**, **II**, and **1**−**4** under identical, or at least very similar, reaction conditions are compiled in Table 4 (for details see footnotes to Table 4). Due to the very poor conversion, the results obtained using MPG as the substrate (Table 2, entries 33−35) have not been included. It is clear that, for ligands **1**−**4**, the homoannularly bridged diphosphine **1** performs best. Only in the case where ETPY was used as the substrate, with a hydrogen pressure of 40 bar, did ligand **2** give a slightly better, though broadly comparable, ee (50 versus 44%, entries 28 and 30, Table 2). As mentioned above, ligands **1** and **2** worked equally well in the hydrogenation of MEAI.

The results for the olefin substrates MAC, MCA, and DMI are best suited for comparison since, in almost all cases, the conversion was quantitative and the enantioselectivities cover a wide range from 2 to 86%. Except in the case of **2** and MCA, the ee values for the homoannularly bridged ligands **1** and **2** are always higher than those of the heteroannular ligands **3** and **4**. The data obtained for the ketones are less informative since for most ligands, including Josiphos, these hydrogenation reactions suffer from both low conversion and

Table 4. Enantioselectivities (%) Obtained with Ligands I, II, and 1−4 under Comparable Reaction Conditions

substrate	I	II	1	2	3	4
MAC[a]	**84**		**71**	21	**35**[f]	11
MCA[b]	**25**		**55**	2	**32**	26
DMI[a]	**99**	97	**86**	83	**63**	43
ETPY[c]	**50**	9	**41**	6		
KPL[d]	**33**	6	**55**	47	**17**	n.d.[g]
MEAI[e]	**73**		**73**	73	**32**	0

[a] 1 bar H_2, 18 °C. [b] 6 bar H_2, 25 °C. [c] 80 bar H_2, 0 °C. [d] 50 bar H_2, 25 °C. [e] 80 bar H_2, 25 °C. [f] 1 bar H_2, 25 °C. [g] Not determined because of low conversion.

low to moderate ee values. In the reaction with KPL, ligands **1** and **2** led to comparable ee values, while with **3** the enantioselectivity dropped. In addition, the strong pressure dependence in these cases makes conclusions less reliable. However, a clear trend was observed in the hydrogenation of imine MEAI. As in the case of the olefin substrates, the homoannular ligands **1** and **2** gave the best results, while the heteroannularly bridged ligands **3** and **4** performed rather poorly. Interestingly, the ee value obtained with ligands **1** and **2** was identical to that obtained with Josiphos (**I**).

In a stricter sense, the influence of changes in the ligand backbone can only be judged by studying a set of ligands with identical functional groups like, for example, **I** (Josiphos), **1**, and **3** (see results printed in bold in Table 4). In the majority of reactions, the heteroannularly bridged ligand **3** performs worst, while the homoannular backbone of **1** seems better suited for the catalysis reactions tested here. In a few cases—although only in the range of low to moderate enantioselectivity—ligand **1** works even better than Josiphos.

Concluding Remarks

In summary, we have synthesized and characterized four new homo- and heteroannularly bridged diphosphine ligands and tested their performance in asymmetric enantioselective hydrogenations of olefins, ketones, and one imine. Generally, the homoannularly bridged Josiphos analogue **1** performed best, giving up to 90.6% ee in the rhodium-catalyzed hydrogenation of dimethyl itaconate and a very promising 73% ee in the iridium-catalyzed hydrogenation of 2-ethyl-*N*-(2-methoxy-1-methylethylidene)-6-methylbenzeneamine (MEAI).

In general, the results of catalytic enantioselective reactions depend on a variety of often strongly related parameters, and therefore, correlations of single parameters (such as structural parameters) with results such as enantioselectivity must be treated with caution. However, the results obtained, particularly with Josiphos, **1**, and **3**, support the view that catalysts expected to perform successfully with different substrates, or even in a diversity of different reactions, require a controlled flexibility rather than very stiff ligand backbones.

Experimental Section

General Comments. NMR spectra were recorded on a Bruker DPX-400 spectrometer in $CDCl_3$ (unless stated otherwise). Chemical shifts are given relative to TMS (^{1}H NMR), $CDCl_3$ (^{13}C NMR), and 85% H_3PO_4 (^{31}P NMR). The coupling constants in ^{13}C spectra are due to ^{13}C−^{31}P coupling. In ^{1}H NMR data d, t, and q refer to doublet, triplet, and quartet, respectively, and q-C in ^{13}C NMR data stands for quaternary carbon atom. Melting points were determined on a Kofler melting point apparatus and are uncorrected. Mass spectra were recorded on a Finnigan MAT 8230 spectrometer (EI). HPLC was carried out on a Hewlett-Packard HP1100 liquid chromatograph; GCs were measured on a Fisons Series 8000 instrument equipped with an FID. CD spectra were recorded on a Jobin Yvon (CD 6) dichrograph, and optical rotations were measured on a Perkin-Elmer 241 polarimeter. Elemental analyses were performed at Mikroanalytisches Laboratorium der Universität Wien. All reactions required inert conditions and were carried out under an argon atmosphere using standard Schlenk techniques. All solvents were dried by standard procedures and distilled before use. Chromatographic separations were performed under gravity either on silica gel (Merck, 40−62μ) or on alumina (Merck, activity II−III, 0.063−0.200 mm). Petroleum ether with a boiling range of 55−65 °C was used for chromatography.

(R_c,S_p)-[η^5-Cyclopentadienyl][η^5-4-dicyclohexylphosphino-3-diphenylphosphino)-4,5,6,7-tetrahydro-1*H*-indenyl]iron(II) (1). To a degassed solution of (−)-(R_c,S_p)-aminophosphine **8** (1.2 g, 2.57 mmol) in freshly distilled acetic acid (23 mL) was added dicyclohexylphosphine (0.6 mL, 3 mmol). The solution was stirred at 90 °C for 5 h. The mixture was cooled to room temperature, and the solvent was evaporated under reduced pressure. The residue was purified by chromatography on alumina (25 × 3 cm) under inert conditions. Excess dicyclohexylphosphine was eluted with petroleum ether, and the product was subsequently eluted with petroleum ether/chloroform, 8/2. Crystallization from CH_2Cl_2 and hexane at 0 °C afforded 529 mg (0.87 mmol, 68%) of orange crystals. Mp: decomposition starts at 64 °C, melting range from 73 to 77 °C. ^{1}H NMR: δ 0.57−0.70 (m, 2H), 0.94−1.32 (m, 10H), 1.37−1.58 (m, 6H), 1.64−1.81 (m, 6H), 1.87−1.95 (m, 1H), 2.14−2.22 (m, 1H), 2.27 (ddd, J_1 = 5.5 Hz, J_2 = 10.0 Hz, J_3 = 15.1 Hz, 1H), 2.59 (ddd, J_1 = J_2 = 5.0 Hz, J_3 = 15.1 Hz, 1H), 3.43 (dd, J_1 = J_2 = 8.5 Hz, 1H), 3.72 (s, 5H, Cp), 3.90 (d, J = 2.5 Hz, 1H, Cp), 4.24 (d, J = 2.0 Hz, 1H, Cp), 7.14−7.23 (m, 3H, Ph), 7.30−7.36 (m, 5H, Ph), 7.61−7.66 (m, 2H, Ph). ^{13}C NMR: δ 23.44 (CH_2), 25.68 (CH_2), 26.49 (CH_2), 26.83 (CH_2), 27.03 (CH_2), 27.53 (d, J = 8.4 Hz, CH_2), 27.68 (d, J = 4.6 Hz, CH_2), 27.77 (d, J = 4.6 Hz, CH_2), 27.94 (d, J = 6.9 Hz, CH_2), 29.83 (d, J = 26.0 Hz, CH), 30.26 (d, J = 14.5 Hz, CH_2), 30.80 (d, J = 9.2 Hz, CH_2), 61.52 (d, J = 12.2 Hz, CH_2), 31.78 (d, J = 24.5 Hz, CH), 31.84 (CH), 34.13 (d, J = 22.2 Hz, CH), 68.43 (Cp), 70.36 (d, J = 4.6 Hz, Cp), 71.36 (Cp), 71.74 (dd, J_1 = 3.1 Hz, J_2 = 4.6 Hz, q-Cp), 89.07 (dd, J_1 = 2.3 Hz, J_2 = 4.6 Hz, q-Cp), 95.62 (dd, J_1 = 17.6 Hz, J_2 = 24.5 Hz, q-Cp), 127.26 (Ph), 127.72 (d, J = 6.9 Hz, Ph), 127.98 (d, J = 7.7 Hz, Ph), 128.78 (Ph), 133.54 (dd, J_1 = 1.5 Hz, J_2 = 17.6 Hz, Ph), 136.28 (d, J = 23.0 Hz, Ph), 140.88 (dd, J_1 = 11.5 Hz, J_2 = 14.5 Hz, q-Ph), 142.77 (dd, J_1 = 1.5 Hz, J_2 = 8.4 Hz, q-Ph). ^{31}P NMR: δ −24.86 (d, J = 123.4 Hz), 18.17 (d, J = 123.4 Hz). MS m/z (%): 620.4 (5.7, M^+), 536.8 (68.8), 422.0 (100), 236.9 (29.8), 183.0 (14.4), 83.0 (39.5). High-resolution mass: calcd for $C_{38}H_{46}FeP_2$, 620.2424; found, 620.2439. Anal. Calcd for $C_{38}H_{46}FeP_2$: C, 73.55; H, 7.47; P, 9.98. Found: C, 73.70; H, 7.52; P, 10.05. $[\alpha]^{20}$ (nm): −427° (589), −455° (578), −581° (546) (c 0.5, $CHCl_3$). CD: $\Delta\epsilon$ (nm) −3.91 (279), 0.44 (342), −1.35 (441) (c 1 × 10^{-4}, CH_2Cl_2).

(R_c,S_p)-[η^5-Cyclopentadienyl][η^5-3,4-bis(diphenylphosphino)-4,5,6,7-tetrahydro-1*H*-indenyl]iron(II) (2). The same protocol as described for **1** was used with the following quantities: (−)-(R_c,S_p)-aminophosphine **8** (600 mg, 1.28 mmol), freshly distilled acetic acid (10 mL), and diphenylphosphine (0.24 mL, 1.4 mmol). The solution was stirred at 90 °C for 4 h. Crystallization from CH_2Cl_2 and hexane at 0 °C yielded 529 mg (0.87 mmol, 68%) of orange crystals. Mp: decomposition starts at 95 °C, melting range from 102 to 107 °C. ^{1}H NMR: δ 1.38−1.45 (m, 1H), 1.74−1.85 (m, 2H), 1.93−2.00 (m, 1H),

2.16 (ddd, J_1 = 5.9 Hz, J_2 = 8.9 Hz, J_3 = 15.3 Hz, 1H), 2.55 (ddd, $J_1 = J_2$ = 4.5 Hz, J_3 = 15.3 Hz, 1H), 3.78 (s, 5H, Cp), 3.89−3.92 (m, 1H), 3.93 (d, J = 2.5 Hz, 1H, Cp), 4.34 (d, J = 2.5 Hz, 1H, Cp), 6.91−7.04 (m, 5H, Ph), 7.06−7.11 (m, 2H, Ph), 7.13−7.20 (m, 3H, Ph), 7.28−7.37 (m, 6H, Ph), 7.24−7.46 (m, 2H, Ph), 7.60−7.65 (m, 2H, Ph). ^{13}C NMR: δ 22.68 (CH_2), 22.37 (CH_2), 25.73 (d, J = 3.1 Hz, CH_2), 33.85 (d, J = 21.4 Hz, CH), 68.96 (Cp), 70.59 (d, J = 3.8 Hz, Cp), 71.48 (Cp), 71.95 (dd, J_1 = 3.1 Hz, J_2 = 9.9 Hz, q-Cp), 89.75 (dd, J_1 = 2.3 Hz, J_2 = 5.4 Hz, q-Cp), 93.19 (dd, J_1 = 19.5 Hz, J_2 = 25.3 Hz, q-Cp), 127.24 (Ph), 127.61 (d, J = 6.1 Hz, Ph), 127.85 (Ph), 128.06 (d, J = 5.4 Hz, Ph), 128.15 (d, J = 7.7 Hz, Ph), 128.46 (d, J = 5.4 Hz, Ph), 128.45 (Ph), 129.08 (Ph), 132.79 (d, J = 1.5 Hz, Ph), 132.95 (d, J = 1.5 Hz, Ph), 133.46 (d, J = 16.8 Hz, Ph), 133.73 (d, J = 19.1 Hz, Ph), 136.24 (d, J = 22.2 Hz, Ph), 137.06 (dd, J_1 = 4.6 Hz, J_2 = 25.2 Hz, q-Ph), 137.91 (dd, J_1 = 2.3 Hz, J_2 = 20.7 Hz, q-Ph), 140.25 (dd, J_1 = 9.9 Hz, J_2 = 12.2 Hz, q-Ph), 141.98 (dd, J_1 = 1.5 Hz, J_2 = 4.6 Hz, q-Ph). ^{31}P NMR: δ −23.63 (d, J = 115.5 Hz), 11.16 (d, J = 115.4 Hz). MS *m*/*z* (%): 607.9 (9.1, M^+), 423.1 (100), 236.9 (9.8), 237.9 (8.3), 182.9 (11.3), 107.9 (14.0). High-resolution mass: calcd for $C_{38}H_{34}FeP_2$, 608.1485; found, 608.1467. Anal. Calcd for $C_{38}H_{34}FeP_2$: C, 75.01; H, 5.63; P, 10.18. Found: C, 73.75; H, 5.79; P, 9.84. $[\alpha]^{20}$ (nm): −381° (589), −401° (578), −487° (546) (*c* 0.5, $CHCl_3$). CD: $\Delta\epsilon$ (nm) −5.27 (280), 1.44 (299), −1.28 (326), −1.08 (441) (*c* 1 × 10^{-4}, CH_2Cl_2).

(R_c,R_p)-1-Diphenylphosphino-2,1′-(1-dicyclohexylphosphinopropanediyl)-ferrocene (3). To a degassed solution of (+)-(R_c,R_p)-aminophosphine **9** (750 mg, 1.65 mmol) in freshly distilled acetic acid (14 mL) was added dicyclohexylphosphine (0.38 mL, 1.9 mmol). The solution was stirred at 100 °C for 18 h. The reaction mixture was cooled to room temperature, and CH_2Cl_2 (15 mL) and saturated $NaHCO_3$ solution (20 mL) were added (vigorous evolution of CO_2). The organic layer was separated, and the aqueous layer was extracted three times with CH_2Cl_2. The combined organic layers were washed until neutral with saturated $NaHCO_3$ solution and water and dried over $MgSO_4$. The solvent was evaporated, and the residue was purified by chromatography on silica ($CHCl_3$). Crystallization from CH_2Cl_2 and hexane afforded 846 mg (1.42 mmol, 86.4%) of yellow crystals. Mp: 108−110 °C. ^{1}H NMR: δ 0.5−1.85 (m, 23H), 2.10−2.25 (m, 2H), 2.50−2.56 (m, 1H), 2.85−2.98 (m, 1H), 3.47 (m, 1H, Cp), 3.82 (m, 1H, Cp), 3.85 (m, 1H, Cp), 4.00 (m, 1H, Cp), 4.12 (m, 1H, Cp), 4.18 (m, 1H, Cp), 4.22 (m, 1H, Cp), 7.18−7.35 (m, 8H, Ph), 7.42−7.47 (m, 2H, Ph). ^{13}C NMR: δ 25.2 (d, J = 9.9 Hz, CH_2), 26.5 (d, J = 8.4 Hz, CH_2), 27.9 (d, J = 16.8 Hz, CH_2), 28.0 (CH_2, 2H), 28.2 (d, J = 3.1 Hz, CH_2), 28.30 (CH_2), 28.36 (d, J = 3.1 Hz, CH_2), 30.53 (d, J = 3.1 Hz, CH_2), 30.96 (d, J = 22.9 Hz, CH_2), 31.48 (d, J = 19.1 Hz, CH), 33.28 (d, J = 24.4 Hz, CH), 33.66 (d, J = 21.4 Hz, CH_2), 34.69 (d, J = 18.3 Hz, CH), 39.14 (dd, J_1 = 10.7 Hz, J_2 = 25.2 Hz, CH_2), 67.63 (Cp), 69.48 (Cp), 69.82 (Cp), 71.57 (Cp), 71.59 (Cp), 73.91 (d, J = 15.3 Hz, q-Cp), 74.44 (d, J = 4.6 Hz, Cp), 75.04 (d, J = 3.8 Hz, Cp), 86.82 (q-Cp), 92.46 (dd, J_1 = 12.2 Hz, J_2 = 22.1 Hz, q-Cp), 127.60 (d, J = 9.2 Hz, Ph), 127.72 (Ph), 127.76 (d, J = 8.1 Hz, Ph), 128.35 (Ph), 133.13 (d, J = 19.1 Hz, Ph), 134.72 (d, J = 20.6 Hz, Ph), 138.69 (dd, J_1 = 5.3 Hz, J_2 = 13.0 Hz, q-Ph), 139.99 (d, J = 7.6 Hz, q-Ph). ^{31}P NMR: δ −23.77 (d, J = 72.7 Hz), 9.64 (d, J = 72.7 Hz). MS *m*/*z* (%): 606 (8.1, M^+), 523 (100), 410 (26.1), 225 (21.5), 129 (30.7), 117 (23.9). High-resolution mass: calcd for $C_{37}H_{44}FeP_2$, 606.2268; found, 606.2281. Anal. Calcd for $C_{37}H_{44}FeP_2$: C, 73.27; H, 7.31; P, 10.21. Found: C, 72.56; H, 7.65; P, 9.83. $[\alpha]^{20}$ (nm): +301° (589), +312° (578), +333° (546) (*c* 0.5, $CHCl_3$). CD: $\Delta\epsilon$ (nm) 10.67 (243), 8.51 (279), −1.05 (421) (*c* 1 × 10^{-4}, CH_2Cl_2).

(R_c,R_p)-1-Diphenylphosphino-2,1′-(1-diphenylphosphinopropanediyl)ferrocene (4). The same protocol as described for **3** was used with the following quantities: (+)-(R_c,R_p)-aminophosphine **9** (2 g, 4.415 mmol) in freshly distilled acetic acid (36 mL) and diphenylphosphine (0.8 mL, 4.6 mmol). The solution was stirred at 100 °C for 18 h. Chromatographic purification on silica (petroleum ether/chloroform, 8/2). Final crystallization from CH_2Cl_2 and hexane afforded 2.042 g (3.44 mmol, 78%) of orange crystals. Mp: 229−232 °C. ^{1}H NMR: δ 1.60 (dd, $J_1 = J_2$ = 14.0 Hz, 1H), 2.06−2.49 (m, 1H), 2.46 (ddd, J_1 = 2.5 Hz, J_2 = 4.0 Hz, J_3 = 15.3 Hz, 1H), 2.73−2.78 (m, 1H), 2.93−3.05 (m, 1H), 3.43−3.45 (m, 1H, Cp), 3.72 (s, 1H, Cp), 3.78−3.81 (m, 1H, Cp), 4.03−4.04 (m, 1H, Cp), 4.09 (t, J = 2.2 Hz, 1H, Cp), 4.20−4.22 (m, 1H, Cp), 4.26 (s, 1H, Cp), 7.02−7.12 (m, 8H, Ph), 7.13−7.20 (m, 2H, Ph), 7.24−7.30 (m, 6H, Ph), 7.43−7.52 (m, 4H, Ph). ^{13}C NMR: δ 25.32 (d, J = 10.7 Hz, CH_2), 37.55 (dd, J_1 = 3.0 Hz, J_2 = 20.6 Hz, CH), 38.48 (dd, J_1 = 10.7 Hz, J_2 = 25.2 Hz, CH_2), 67.76 (Cp), 69.68 (Cp), 70.05 (Cp), 71.48 (d, J = 4.58 Hz, Cp), 71.66 (Cp), 74.12 (q-Cp), 74.31 (d, J = 3.8 Hz, Cp), 76.21 (d, J = 3.0 Hz, Cp), 87.34 (q-Cp), 90.76 (d, J = 17.1 Hz, q-Cp), 127.73 (Ph), 128.03 (d, J = 6.9 Hz, Ph), 128.17 (d, J = 7.6 Hz, Ph), 128.65 (d, J = 4.6 Hz, Ph), 128.70 (Ph), 129.06 (d, J = 10.0 Hz, Ph), 133.46 (d, J = 19.0 Hz, Ph), 134.01 (d, J = 42.1 Hz, Ph), 134.01 (Ph), 135.45 (d, J = 21.4 Hz, Ph), 137.75 (d, J = 15.3 Hz, q-Ph), 139.11 (dd, J_1 = 5.4 Hz, J_2 = 12.2 Hz, q-Ph), 140.31 (dd, J_1 = 3.1 Hz, J_2 = 21.4 Hz, q-Ph), 140.84 (d, J = 6.9 Hz, q-Ph). ^{31}P NMR: δ −6.63 (d, J = 79.7 Hz), −22.27 (d, J = 79.7 Hz). MS *m*/*z* (%): 594 (47.2, M^+), 517 (14.8), 409 (100), 331.7 (20.9), 242 (11.7), 223.8 (34.3), 198.8 (36.8), 128.9 (21.1), 95.9 (37.3), 62.9 (21.1). High-resolution mass: calcd for $C_{37}H_{32}FeP_2$, 594.1329; found, 594.1352. Anal. Calcd for $C_{37}H_{32}FeP_2$: C, 74.76; H, 5.43; P, 10.42. Found: C, 74.49; H, 5.64; P, 10.69. $[\alpha]^{20}$ (nm): +233° (589), +238° (578), +240° (546) (*c* 0.9, $CHCl_3$). CD: $\Delta\epsilon$ (nm) −5.14 (243), −5.16 (251), 5.72 (281), −1.23 (428) (*c* 1 × 10^{-4}, CH_2Cl_2).

(R_c,S_p)-[η^5-Cyclopentadienyl][η^5-4-hydroxy-4,5,6,7-tetrahydro-1*H*-indenyl]iron(II) (6). To a suspension of $LiAlH_4$ (0.41 g, 10.25 mmol) in dry ether (100 mL) was added dropwise a solution of ketone (S_p)-**5** (4.04 g, 20.4 mmol) in diethyl ether at room temperature. The reaction mixture was stirred at room temperature for 2 h, a second portion of $LiAlH_4$ (100 mg, 2.64 mmol) was added, and the reaction mixture was heated under reflux for an additional 30 min. After complete conversion (TLC: silica, CH_2Cl_2), water (100 mL) was added slowly at 0 °C. The organic layer was separated, and 10% H_2SO_4 was carefully added to the aqueous layer until all $Al(OH)_3$ had dissolved. The aqueous layer was extracted with ether (2 × 50 mL), and the combined organic layers were washed with water (2 × 50 mL). The organic phase was dried over $MgSO_4$, the solvent was evaporated, and the residue was purified by chromatography on silica (CH_2Cl_2) to yield 4.01 g (20.05 mmol, 98%) of the desired product. ^{1}H NMR: δ 1.59 (m, 2H), 1.83 (m, 2H), 2.18 (m, 1H), 2.35 (m, 1H), 2.60 (m, 1H), 4.01 (s, 5H, Cp), 4.09 (m, 1H, Cp), 4.29 (m, 1H, Cp), 4.93 (m, 1H, Cp). ^{13}C NMR: δ 19.67 (CH_2), 24.48 (CH_2), 32.98 (CH_2), 65.26 (CH), 65.98 (Cp), 66.24 (Cp), 67.25 (Cp), 69.56 (5 Cp), 85.17 (q-Cp), 85.50 (q-Cp). MS *m*/*z* (%): 256 (100, M^+), 238 (96), 188 (37), 172 (97), 121 (87), 115 (95). Anal. Calcd for $C_{14}H_{16}FeO$: C, 65.63; H, 6.25. Found: C, 65.64; H, 6.42. $[\alpha]^{20}$ (nm): −129° (589) (*c* 1.35, EtOH).

(R_c,S_p)-[η^5-Cyclopentadienyl][η^5-4-*N*,*N*-(dimethylamino)-4,5,6,7-tetrahydro-1*H*-indenyl]iron(II) (7). To a suspension of $AlCl_3$ (4.08 g, 30.6 mmol) in 1,2-dichloroethane (100 mL) was added an excess of dimethylamine at 0 °C (an excess of amine is essential, otherwise elimination of water becomes the predominant reaction). To the clear solution was added dropwise a solution of (R_c,S_p)-**6** (4.04 g, 15.8 mmol) in 1,2-dichloroethane (100 mL) at 0 °C. The reaction mixture was stirred for 10 h at 60−65 °C (the conversion was monitored by TLC, alumina, petroleum ether/triethylamine, 9/1), and 0.2 N KOH (100 mL) was added. The organic layer was separated, and the aqueous layer was extracted with 1,2-dichloroethane (3 × 30 mL). The combined organic layers were washed with water (2 × 50 mL) and dried over $MgSO_4$, and the solvent was evaporated. Purification of the residue by chromatography on alumina (petroleum ether/triethylamine, 9/1) afforded 3.30 g

Table 5. Crystallographic Data for (R_c,S_p)-1, (R_c,S_p)-2, (S_c,S_p)-3·CH_2Cl_2, and (R_c,R_p)-4

	(R_c,S_p)-**1**,	(R_c,S_p)-**2**	(S_c,S_p)-**3**·CH_2Cl_2	(R_c,R_p)-**4**
formula	$C_{38}H_{46}FeP_2$	$C_{38}H_{34}FeP_2$	$C_{38}H_{46}Cl_2FeP_2$	$C_{37}H_{32}FeP_2$
fw	620.54	608.44	691.44	594.42
cryst size, mm	0.50 × 0.34 × 0.12	0.50 × 0.35 × 0.25	0.80 × 0.40 × 0.18	0.70 × 0.50 × 0.40
cryst syst	orthorhombic	orthorhombic	monoclinic	orthorhombic
space group	$P2_12_12_1$ (No. 19)	$P2_12_12_1$ (No. 19)	$P2_1$ (No. 4)	$P2_12_12_1$ (No. 19)
a, Å	9.791(4)	14.484(5)	10.586(2)	10.441(3)
b, Å	20.805(9)	14.630(5)	15.589(4)	11.251(3)
c, Å	32.548(14)	15.274(6)	10.832(2)	25.416(6)
β, deg			103.16(1)	
V, Å^3	6630(5)	3237(2)	1740.6(6)	2985.7(14)
Z	8	4	2	4
ρ_{calc}, g cm^{-3}	1.243	1.249	1.319	1.322
T, K	299(2)	298(2)	295(2)	298(2)
μ, mm^{-1}(Mo Kα)	0.58	0.59	1.32	0.64
F(000)	2640	1272	728	1240
θ_{max}, deg	25	25	30	30
no. of rflns measd	73 431	34 568	25 379	47 786
no. of unique rflns	11 625	5700	9673	8674
no. of rflns $I > 2\sigma(I)$	9600	4957	8548	7964
no. of params	739	380	389	361
R_1 [$I > 2\sigma(I)$][a]	0.040	0.041	0.033	0.034
R_1 (all data)[a]	0.057	0.056	0.040	0.038
wR_2 (all data)[a]	0.091	0.114	0.085	0.083
diff Fourier peaks min/max, e Å^{-3}	−0.16/0.24	−0.31/0.63	−0.38/0.43	−0.20/0.24
Flack absolute structure param	−0.007(12)	−0.05(2)	0.005(10)	0.002(10)

[a] $R_1 = \sum||F_o| - |F_c||/\sum|F_o|$, $wR_2 = [\sum(w(F_o^2 - F_c^2)^2)/\sum(w(F_o^2)^2)]^{1/2}$.

(11.7 mmol, 74%) of product **7**. ^{1}H NMR: δ 1.25 (m, 1H), 1.88 (m, 3H), 2.16 (m, 1H), 2.19 (s, 6H), 2.50 (m, 1H), 3.98 (m, 1H, Cp), 4.00 (s, 5H, Cp), 4.05 (m, 1H, Cp), 4.10 (dd, J_1 = 5 Hz, J_2 = 11 Hz, 1H, Cp), 4.33 (m, 1H, Cp). ^{13}C NMR: δ 22.04 (CH_2), 22.13 (CH_2), 24.96 (CH_2), 40.37 (CH_3), 61.34 (CH), 65.16 (Cp), 65.40 (Cp), 65.96 (Cp), 69.50 (5 Cp), 85.45 (q-Cp), 86.23 (q-Cp). MS m/z (%): 283 (38, M^+), 237 (67), 172 (41), 121 (70), 115 (67), 56 (100). [α]^{20} (nm): −148° (589), (c 1.34, EtOH).

(R_c,S_p)-[η^5-Cyclopentadienyl][η^5-4-*N*,*N*-(dimethylamino)-3-diphenylphosphino)-4,5,6,7-tetrahydro-1*H*-indenyl]iron(II) (8). To a degassed solution of (R_c,S_p)-**7** (3.02 g, 10.7 mL) in diethyl ether (70 mL) was added slowly at 0 °C a 1.6 N solution of *n*-BuLi in ether (9.9 mL, 15.8 mmol). The solution was stirred at room temperature for 10 h, $ClPPh_2$ (3.7 mL, 20.4 mmol) was added, and the solution was stirred for an additional 12 h. Saturated aqueous $NaHCO_3$ solution (50 mL) was added, the organic layer was separated, and the aqueous layer was extracted with ether (3 × 20 mL). The combined organic layers were washed with water (2 × 30 mL) and dried over $MgSO_4$. The solvent was evaporated, and the residue was purified by chromatography on silica (methanol/$CHCl_3$, 2/8) to afford 3.53 g (7.56 mmol, 70.7%) of product **8**. ^{1}H NMR: δ 1.42 (m, 1H), 1.62 (s, 6H), 1.83 (m, 2H), 1.97 (m, 1H), 2.22 (m, 1H), 2.48 (m, 1H), 3.72 (m, 1H, Cp), 3.89 (s, 5H, Cp), 4.20 (d, J = 2 Hz, 1H, Cp), 4.33 (dd, J_1 = 6 Hz, J_2 = 8.5 Hz, 1H, Cp), 7.15−7.70 (m, 10H, Ph). ^{13}C NMR: δ 19.67 (CH_2), 22.41 (CH_2), 25.40 (CH_2), 39.51 (CH_3), 59.52 (CH), 67.07 (Cp), 69.72 (d, J = 6 Hz, Cp), 70.91 (5 Cp), 73.80 (d, J = 8 Hz, q-Cp), 89.68 (d, J = 4 Hz, q-Cp), 92.25 (d, J = 20.3 Hz, q-Cp), 127.40 (Ph), 127.45 (d, J = 7.4 Hz, Ph), 127.65 (d, J = 7.1 Hz, Ph), 128.24 (Ph), 132.88 (d, J = 20.68 Hz, Ph), 134.92 (d, J = 21.4 Hz, Ph), 139.40 (d, J = 12 Hz, q-Ph), 140.70 (d, J = 10 Hz, q-Ph). ^{31}P NMR: δ −22.47. MS m/z (%): 467 (41, M^+), 422 (89), 357 (13), 276 (24), 237 (100), 220 (41), 183 (39), 121 (61). Anal. Calcd for $C_{28}H_{30}FeNP$: C, 71.90; H, 6.42; N, 3.0. Found: C, 71.84; H, 6.61; N, 2.92. [α]^{20} (nm): −423° (589) (c 0.384, CH_2Cl_2).

Standard Procedure for Hydrogenation Reactions. The substrate (2.5 mmol; 12.7 mmol in the case of MEAI) and the catalyst (formed in situ, for details see Tables 1−4) were dissolved separately in 5 mL of the solvent under argon (total volume: 10 mL). The catalyst solution was stirred for 15 min. Both the catalyst and the substrate solution were transferred via a steel capillary into a 180 mL thermostated glass reactor or a 50 mL stainless steel autoclave. The inert gas was then replaced by hydrogen (three cycles), and the pressure was set. After completion of the reaction (total reaction times 16−66 h), the conversion was determined by gas chromatography, and the product was recovered quantitatively after filtration of the reaction solution through a plug of silica to remove the catalyst. The enantiomeric purity of the product was determined either by gas chromatography or by HPLC (see footnotes in Tables 1−3).

X-ray Structure Determination of (R_c,S_p)-1, (R_c,S_p)-2, (S_c,S_p)-3·CH_2Cl_2, and (R_c,R_p)-4. Crystals of (R_c,S_p)-**1**, (R_c,S_p)-**2**, (S_c,S_p)-**3**·CH_2Cl_2, and (R_c,R_p)-**4** were obtained by diffusion of diethyl ether into CH_2Cl_2 solutions of the compound in question. Crystal data and experimental details are summarized in Table 5. X-ray data were collected on a Bruker Smart CCD area detector diffractometer (graphite-monochromated Mo Kα radiation, λ = 0.71073 Å, 0.3° ω-scan frames covering complete spheres of the reciprocal space). Corrections for Lorentz and polarization effects, for crystal decay, and for absorption were applied. All structures were solved by direct methods using the program SHELXS97.[21] Structure refinement on F^2 was carried out with the program SHELXL97.[21] All non-hydrogen atoms were refined anisotropically. Hydrogen atoms were inserted in idealized positions and were refined riding with the atoms to which they were bonded.

Acknowledgment. We gratefully acknowledge the Subdirección General de Cooperación Internacional for an "Acción Integrada" project (HU-1999-0017) as well as Österreichischer Akademischer Austauschdienst for the "Acción Integrada" project 18/2000. This work was kindly supported by the Dirección General de Enseñanza Superior e Investigaciones Científicas, Spain (Grant No. PB98-0315), and by Österreichische Nationalbank, Austria (project 7516).

Supporting Information Available: Tables giving crystal data of **1**−**4** as well as details of the structure determination, non-hydrogen atomic coordinates, bond distances and angles, anisotropic thermal parameters, and hydrogen coordinates with isotropic displacements parameters. This material is available free of charge via the Internet at http://pubs.acs.org.

OM0107439

(21) Sheldrick, G. M. *SHELX-97*: Program System for the Solution and Refinement of Crystal Structures; University of Göttingen: Germany, 1997.